

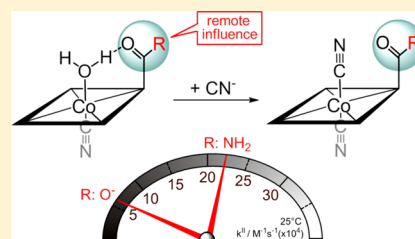
Controlling Binding Dynamics of Corrin-Based Chemosensors for Cyanide

Balz Aebli, Christine Männel-Croisé, and Felix Zelder*

Department of Chemistry, University of Zürich, Winterthurerstrasse 190, 8057 Zürich, Switzerland

Supporting Information

ABSTRACT: This paper describes a strategy to control the binding dynamics between cyanide and aquacyanocorrinoids on the molecular level. Aquacyanocorrinoids represent an important class of chemosensors and convert upon cyanide coordination to the corresponding dicyano derivatives. Structure–reactivity relationships were investigated for the first time by synthesizing and studying three diastereomerically pure aquacyanocorrinoids differing either in the configuration of the axially bound ligands or in the nature of remote side chains located at the periphery of the corrin macrocycle. Substitution of cobalt-coordinated water with cyanide was investigated using stopped-flow measurements between 5 and 30 °C, and second order rate constants and activation parameters were determined. In particular, it is demonstrated that the binding kinetics depend not only on (i) the configuration at the central metal center but also on (ii) the remote structural modifications of the macrocycle.



INTRODUCTION

The development of chemosensors for the colorimetric and fluorometric detection of anions is a fast growing discipline.^{1–3} Analytes of environmental and medicinal concern attract particular interest, and a plethora of new reagents for fluoride and cyanide detection has been developed in the last years.^{3–6} These compounds sense cyanide either by (i) hydrogen bonding⁷ or by (ii–iv) bond forming reactions with electrophilic (ii) carbon,^{8,9} (iii) boron,^{10,11} or (iv) metal centers.^{12,13} Indeed, enormous progress in sensitivity, selectivity, water compatibility, and detection in biological samples has been observed.^{4,5,14,15} Our group reported the first methods for rapid “naked-eye” detection of cyanide in plants and blood with corrin-based chemosensors.^{16–18} Despite important developments in the design of new chemosensors, rather little attention is paid to systematic studies of structure–reactivity relationships in a defined system. One of the few exceptions in the field of cyanide and fluoride sensing was reported on cationic boron-based reagents by Gabbai and co-workers.¹⁹ It was demonstrated that remote structural modifications offer a handle to modulate effectively the sensitivity and selectivity of the receptor.^{20,21} Distinct cyanide affinities were also observed by our group for cyanide coordination to “incomplete” aquacyanocorrinoids with different side chains at the periphery of the molecule.²² These derivatives convert upon cyanide binding to the corresponding dicyano compounds.²³ The implementation of seven negatively charged carboxylates instead of neutral amides or esters lowers the affinity of cyanide by a factor of 10.²² One of these derivatives, aquacyanocobyrinic acid, was also tested for cyanide binding under pseudo first order conditions in a previous kinetic study.¹⁸ However, the reagent was applied as a diastereomeric mixture of “upper” (β) cyano, “lower” (α) aqua and “upper” (β) aqua, “lower” (α) cyano

corrinoids due to difficulties in separation. Second order rate constants of 4200 and 15600 M⁻¹ s⁻¹ were derived from the experimental data, and we supposed a distinct speed of cyanide coordination to the diastereomers.¹⁸ This observation was in contrast to a pioneering kinetic study of the reaction between cyanide and aquacyanocobinamide, reporting undistinguishable rates for both diastereomers.²⁴ In addition, the results were subsequently challenged by a study of Chemaly, Marques, and co-workers suggesting that the rate of substitution of water by cyanide at both faces of aquacyanoheptamethyl cobyrinic acid are indistinguishable.²⁵ Unfortunately, all of these experiments were performed with a diastereomeric mixture hampering a clear-cut interpretation.

To gain a clear picture of cyanide binding to corrinoids,^{26–29} kinetic studies with diastereomerically pure aquacyanocorrinoids differing only in the axial configuration at the cobalt center are desired.

The availability of isomerically pure corrin-based chemosensors also represents the basis for systematic studies of structure–reactivity relationships. This information is required for a better understanding of the system and for further optimization. Of note, favorable kinetics represent also the prerequisite for potential implementations into functional devices.^{16,30–34}

Herein we extend our studies with corrin-based chemosensors for cyanide and report for the first time kinetics of cyanide binding to diastereomerically pure aquacyanocorrinoids with a well-defined axial aquacyano configuration at the cobalt ion, but with distinct side chains at the periphery of the macrocycle (**1**, **2**, **4**; Figure 1). Insights into the influence of (i)

Received: October 21, 2013

Published: February 10, 2014

the stereochemistry at the metal center (**1** vs **2**) and of (ii) remote site chains located at the periphery of the macrocycle (**1** vs **4**) on the binding dynamics were obtained.

EXPERIMENTAL SECTION

All chemicals were obtained from Sigma-Aldrich Corporation or Fluka Chemie AG (Buchs, Switzerland). Vitamin B₁₂ was a generous gift from DSM Nutritional Products AG (Basel, Switzerland). Doubly distilled water and solvents of HPLC or LC-MS quality were used in all experiments.

UV-vis spectra were measured at $T = 21 \pm 1^\circ\text{C}$ with a Cary 50 spectrometer using quartz cells with a path length of 1 cm.

NMR spectra were recorded on a Bruker AV-500 spectrometer (Karlsruhe, Germany). The chemical shifts are given in ppm relative to the signal of residual protons of MeOH-*d*₄ at 4.87 ppm.

Analytical HPLC separations were performed on a Merck-Hitachi L-7000 system and Macherey Nagel Nucleosil C18ec RP columns (5 μm particle size, 100 Å pore size, 250 × 3 mm, flow rate of 0.5 mL/min). Gradient: 0.1% aq TFA versus MeOH (5 to 50 min from 25 to 100% MeOH).

Preparative RP-HPLC separations were performed on a Varian Prostar system equipped with two Prostar 215 pumps, a Prostar 320 UV/Vis detector and Macherey Nagel Nucleosil C18ec RP columns (7 μm particle size, 100 Å pore size, 250 × 40 mm, flow rate of 35 mL/min). Gradient used for compounds **1** and **2**: 0.1% aq TFA versus MeOH (5 to 45 min from 20 to 40% MeOH).

ESI-MS spectra were recorded on a Bruker Esquire HCT instrument. The injection rate for ESI measurements was 3 μL/min with a nebulizer pressure of 10 psi, and a dry gas flow rate of 5 L/min at a gas temperature of 300 K were used.

LC-MS was performed using a Waters Acquity Ultra Performance LC equipped with a Macherey Nagel C18ec RP column (5 μm particle size, 100 Å pore size, 250 × 3 mm, flow rate of 0.3 mL/min). Gradient: 0.1% aq formic acid versus MeOH (5 to 50 min from 25 to 100% MeOH).

Stock solutions of CHES buffer (0.5 M) at pH 9.5 were prepared, and the desired pH values were adjusted by addition of aqueous KOH (2 M).

Stock solutions of KCN (10 mM) and **1**, **2**, and **4** (80 μM) were prepared directly before use. A time-resolved ¹H NMR study with **2** in D₂O at 300 K over a period of 16 h was performed to exclude the possibility of isomerization of the axial ligands prior to kinetic measurements. Less than 1% of isomerization of **2** to **1** within 3.2 hours and less than 6% of isomerization within 16 h was observed. The ratio of **2** to **1** was calculated by comparing the integrals of the characteristic signals of the singlet of H10 of **2** at 6.55 ppm and of **1** at 6.48 ppm. The concentration of CN⁻ at pH 9.5 was calculated with the Henderson-Hasselbalch equation.

Synthesis. Compounds **1** and **2** (Figure 1) were synthesized as their TFA salts as described in the literature.^{35,36} The ¹H NMR spectra of **2** is shown as a representative example in Figure S1. A modified literature procedure was used for the synthesis of **4**.³⁷ Crude **4** was first synthesized from vitamin B₁₂ (100.0 mg, 73.8 μmol) as described in ref 37. Afterward, the crude product (10 mg, 8.5 μmol) was purified by flash chromatography on silica gel (DCM/MeOH 100:2) to yield pure **4** with a β-aqua, α-cyano configuration (3 mg, 2.5 μmol, 13%). A fraction (4 mg, 3.4 μmol, 18%) containing the corresponding α-aqua-β-cyano diastereoisomer of **4** (Partial characterization: (i) DC (silica; CH₂Cl₂, MeOH (10%)): $R_f = 0.31$. (ii) ESI-MS (MeOH) m/z : $[M - H_2O]^+$ calcd for C₅₂H₇₁CoN₅O₁₄, 1048.4; found, 1048.7 (100%). (iii) ¹H NMR (500 MHz, MeOH-*d*₄) δ (ppm): 6.47 (s, 1H), 4.34 (d, $J = 4.5$, 1H), 4.07 (d, $J = 4.5$, 1H)), but additional impurities of **4** (for characterization see below) were also obtained. It has to be noted that the synthesis of the α-aqua-β-cyano diastereomer yielded inconsistent results.

Characterization of Compound 4. DC (silica; CH₂Cl₂, MeOH (10%)): $R_{f(4)} = 0.58$. HPLC: $R_{t(4)} = 27.6$ min. UV-vis: (H₂O) λ_{max} /nm (log ε): 320 (4.01), 354 (4.41), 405 (3.65), 496 (3.92), 526 (3.90). ESI-MS (MeOH) m/z : $[M - H_2O]^+$ calcd for

C₅₂H₇₁CoN₅O₁₄, 1048.4; found, 1048.2 (100%). ¹H NMR (500 MHz, MeOH-*d*₄) δ (ppm): 6.44 (s, 1H), 4.13 (d, $J = 4.5$, 1H), 4.08 (d, $J = 5.0$, 1H), 3.83 (s, 3H), 3.77 (s, 3H), 3.75 (s, 3H), 3.74 (s, 3H), 3.69 (s, 3H), 3.64 (s, 3H), 3.56 (t, $J = 6.0$, 1H), 3.49 (s, 1H), 3.21 (s, 1H), 3.12 (m, 1H), 2.95–1.1 (m, 21H), superimposed by 2.46 (s, 3H), 2.44 (s, 3H), 1.73 (s, 3H), 1.67 (s, 3H), 1.61 (s, 3H), 1.53 (s, 3H), 1.44 (s, 3H), and 1.39 (s, 3H). The configurations of the axial ligands of compounds **1**, **2**, and **4** were verified by analyzing and comparing the characteristic shifts of the protons H3, H10, and H19 as described recently for aquacyanocorrinoids.³⁸

Stopped-Flow Kinetic Measurements. Stopped-flow kinetic measurements were recorded with a SX20 spectrometer from Applied Photophysics, equipped with a xenon lamp and a PDA detector. The temperature was regulated with a water bath. One thousand UV-vis spectra were recorded within either 1.26 s for compound **4** or 1.00 s for compounds **1** and **2**. The kinetic data are averaged values of five experiments for compounds **1** and **2** and of four experiments for compound **4**.

Data Analysis—General Information. Data analysis was performed with an OriginPro 8.5 from Origin Lab Corporation³⁹ and with KinTek Explorer from KinTek Corporation.⁴⁰ OriginPro was used to assess the overall quality of the data and perform single wavelength analysis by fitting mono- or biexponential functions ($A = A_0 + ae^{-k_{\text{obs1}}*t}$, $A = A_0 + ae^{-k_{\text{obs1}}*t} + be^{-k_{\text{obs2}}*t}$). For this data evaluation, the change of absorption at 584 nm for compounds **1** and **2** and at 582 nm for compound **4** was used.

For the data analysis with KinTek Explorer, a stopped-flow measurement (UV-vis spectra) was imported as a wavelength (650–300 nm) by time (0–1.26 or 1.00 s) matrix. This matrix was factorized by singular value decomposition (SVD). A singular value (SV) corresponds to a reactive species identified by SVD. Only SV ≥ 1 were taken into account.

Data Analysis for Kinetic Experiments with 1 or 4. In the KinTek Explorer, the reaction between cyanide and **1** or **4** was defined in the model editor as $A + B = C$.

Example for Kinetic Experiments with 4. The concentrations for the starting conditions ($t = 0$) were defined in the experiment editor as A: $[4] = 40 \mu\text{M}$, B: $[\text{CN}^-] = 307, 613, 920, \text{ or } 1533 \mu\text{M}$ and C: $[5] = 0 \mu\text{M}$. The observed decreasing SV amplitude versus time spectrum was linked to A and the increasing SV amplitude versus time spectrum was linked to C. Four measurements with different concentrations of excess cyanide at a certain temperature were fitted simultaneously (for an example see Figure S2).

Data Analysis for Kinetic Experiments with 2. The reaction was defined in the model editor as $A + B = C$ and $U + B = C$. The concentrations of A and the unknown species U were determined as 96% and 4% of the initial concentration by calculations with averaged values of the prefactors a and b of biexponential fits at 584 nm (OriginPro) at multiple cyanide concentrations and temperatures. Due to the fast reaction kinetics of **2** at higher temperatures, $[\text{CN}^-] = 1533 \mu\text{M}$ was excluded from the fits for the analysis at 20 °C and $[\text{CN}^-] = 920$ and $1533 \mu\text{M}$ were excluded from the fits at 25 and 30 °C.

RESULTS AND DISCUSSION

The conversion of the diastereomerically pure aquacyanocobinamides **1** and **2** with cyanide to the corresponding dicyano derivative **3** was studied under pseudo first order conditions with stopped-flow measurements at pH 9.5 between 5 and 30 °C (Figure 1; Table 1).

The two isomeric receptors **1** and **2** differ only by the nature of the binding pocket, which is defined by the side chains directing either to the upper or lower face of the metal complex as schematically depicted in Figure 2.

The substitution of cobalt-coordinated water of **1** (40 μM) by cyanide (307 μM) to dicyanocobinamide (**3**) is accompanied by a characteristic red shift of the α-, β-, and γ-bands (Figure 2A, Figure 3 inset).

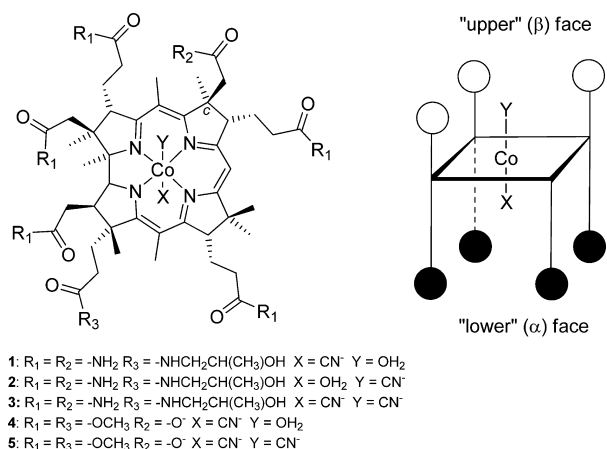


Figure 1. Structural formula (left) and schematic representation (right) of incomplete aquacyanocorrinoids (**1**, **2**, **4**) and the corresponding dicyano forms (**3**, **5**).

The corresponding plot for the change in absorbance at 584 nm is depicted in Figure 3. The kinetic trace can be fitted monoexponentially, yielding $k_{obs(1)}$ of 60.75 s^{-1} . Afterward, kinetic data were collected at different concentrations of cyanide and temperatures and fitted globally using KinTek Explorer Software.

In Table 1, values of k_{11}^{II} are presented, which vary between 4 and $33 \times 10^4 \text{ M}^{-1} \text{ s}^{-1}$. The activation parameters ΔS^{\ddagger} and ΔH^{\ddagger} for the reaction of **1** with cyanide are $50 \text{ JK}^{-1} \text{ mol}^{-1}$ and 58 kJ mol^{-1} , respectively, and were determined from the temperature dependency. The Eyring plot is shown in Figure 4. The positive activation entropy suggests a dissociative interchange mechanism (Table 2).

In contrast to experiments with **1**, the monoexponential fit for the reactions between cyanide and **2** were not completely satisfying (Figure S3). In this case, a biexponential fit offered a slightly better correlation to the experimental data (Figure S4), suggesting the presence of an additional minor unknown corrin species (4%) under the reaction conditions.

The second order rate constants k_{12}^{II} as well as the activation parameters ΔS^{\ddagger} and ΔH^{\ddagger} (Figure 4) for the reaction between **2** and cyanide are summarized in Tables 1 and 2. Cobinamide **2** (Figures 1, 2B) with an α -aqua, β -cyano configuration at the metal center reacts at $25 \text{ }^\circ\text{C}$ with a k_{12}^{II} value of $72 \times 10^4 \text{ M}^{-1} \text{ s}^{-1}$. This is approximately 3 times faster than **1**, which exhibits the inverse configuration of the axial ligands.

This study with pure diastereomers of incomplete aquacyanocorrinoids contradicts some earlier investigations^{24,25} and shows unambiguously that substitutions at both faces of diastereomeric incomplete aquacyanocorrinoids are distinguishable. This kinetic behavior seems to be plausible considering that both diastereomers contain a different environment in

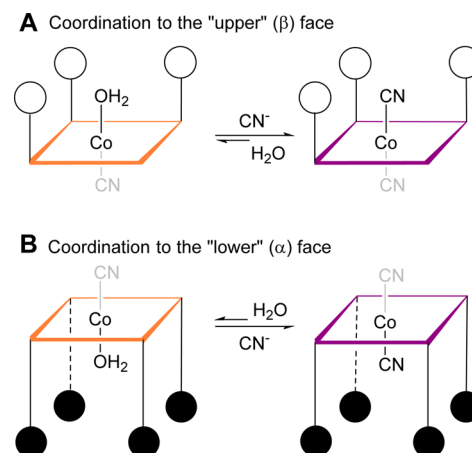


Figure 2. (A) Schematic representation of cyanide coordination to the upper face of incomplete aquacyanocorrinoids. (B) Coordination to the opposite face.

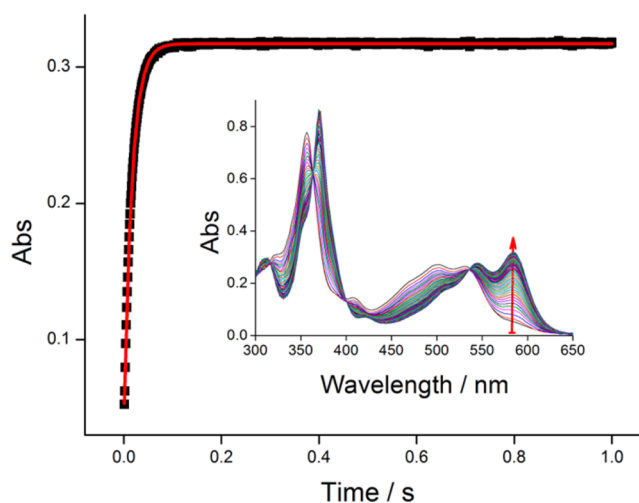


Figure 3. Change in absorbance at 584 nm for the reaction between **1** ($40 \mu\text{M}$) and CN^- ($307 \mu\text{M}$) to **3** at pH 9.5 (CHES buffer 0.1 M) and $25 \text{ }^\circ\text{C}$. It was fitted with a monoexponential function $A = A_0 + ae^{-k_{obs}t}$ (red line). Inset: corresponding UV/vis absorption spectra.

proximity to the metal binding site. Different rate constants were also observed earlier for the coordination of cyanide to the α - and β -forms of protonated base-off aquacyanocobalamin.²⁶ In agreement with our observation, the α -aqua, β -cyano form reacts faster than the β -aqua, α -cyano derivative, but the 1.4 fold enhancement at $25 \text{ }^\circ\text{C}$ is significantly lower than for the corresponding reaction with the incomplete diastereomeric corrinoids **2** and **1** applied in our study (Table 1; $k_{12}^{\text{II}}/k_{11}^{\text{II}} = 3.2$ at $25 \text{ }^\circ\text{C}$).

Table 1. Second Order Rate Constants for the Substitution of Co^{3+} -Bound Water by Cyanide^a

temp ($^\circ\text{C}$)	k_{11}^{II} ($\text{M}^{-1} \text{ s}^{-1} \times 10^4$)	k_{12}^{II} ($\text{M}^{-1} \text{ s}^{-1} \times 10^4$)	k_{14}^{II} ($\text{M}^{-1} \text{ s}^{-1} \times 10^4$)	$k_{12}^{\text{II}}/k_{11}^{\text{II}}$
5 ± 0.1	3.96 ± 0.15	14.35 ± 0.33	1.39 ± 0.03	3.62
10 ± 0.1	6.22 ± 0.25	22.16 ± 0.28	2.03 ± 0.05	3.56
15 ± 0.1	9.83 ± 0.37	34.15 ± 0.32	3.07 ± 0.07	3.47
20 ± 0.1	15.08 ± 0.54	48.93 ± 1.87	4.53 ± 0.11	3.24
25 ± 0.1	22.61 ± 0.95	71.74 ± 3.87	6.52 ± 0.17	3.17
30 ± 0.1	33.22 ± 1.55	97.76 ± 5.17	9.33 ± 0.24	2.94

^aIn the β -position of **1** and **4** (k_{11}^{II} and k_{14}^{II} ; Figure 2A) or in the α -position of **2** (k_{12}^{II} ; Figure 2B).

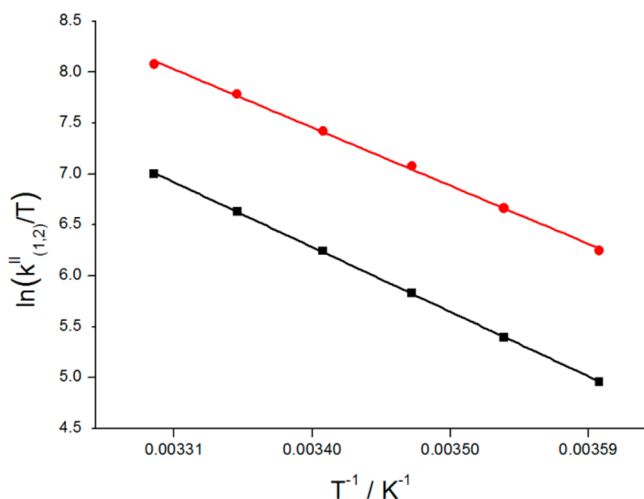


Figure 4. Temperature dependence of k_1^{II} (black) and k_2^{II} (red) for the reactions between cyanide and **1** or **2** is illustrated by an Eyring plot.

Table 2. Activation Parameters for the Reaction between Cyanide and **1**, **2**, or **4**

compd	ΔS^\ddagger ($\text{JK}^{-1} \text{mol}^{-1}$)	ΔH^\ddagger (kJ mol^{-1})
1	50 ± 1	58 ± 1
2	47 ± 5	53 ± 1
4	19 ± 1	51 ± 1

The cobalt-coordinated water directed to the upper (β) face in **1** (Figure 2A) is surrounded by three acetamide side chains instead of four propionamides at the lower (α) face in **2** (Figure 2B). Surprisingly, the apparently stronger shielded metal center of **2** reacts faster with cyanide than **1**.

The influence of the chemosensor's environment on the binding rate was further studied with derivative **4** (Figure 1).³⁷ This corrin derivative contains the same β -aqua, α -cyano configuration at the metal center as **1** but differs in the nature of remote side chains located at the rim of the receptor. As shown in Figure 5, the periphery of the upper face of **4** is decorated with two methylester and one carboxylate functionalities instead of three acetamides in **1**.

Hydrogen bonding interactions between cobalt-coordinated water at the upper (β) position of the macrocycle and the carbonyl moiety at the *c*-side chain have been observed for corrinoids in solution and in the solid state.^{41,42} We speculated

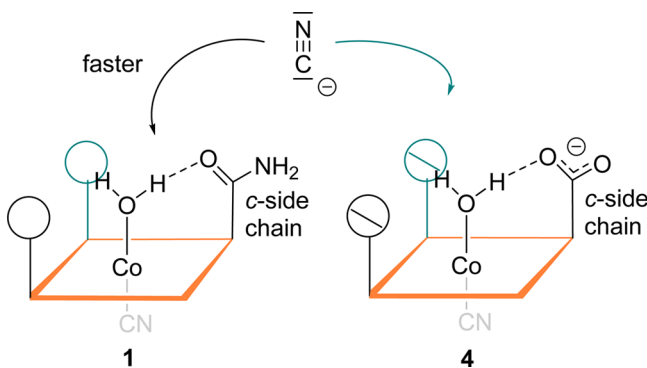


Figure 5. Comparison of cyanide binding to the cobalt binding site of receptor **1** (left) and **4** (right).

therefore that a switch at the *c*-position from an amide in **1** to a negatively charged carboxylate group in **4** would influence cyanide binding, probably also because of repulsive interactions (Figure 5). As observed earlier for **1**, monoexponential fits were satisfying for plots of the reaction between **4** and cyanide. In agreement with our assumption, the second order rate constant k_4^{II} of $6.5 \times 10^4 \text{ M}^{-1} \text{ s}^{-1}$ is approximately 3.5 times slower than that of **1** at 25 °C. Interestingly, an influence is also observed on the activation parameters ΔS^\ddagger and ΔH^\ddagger (Table 2). The less positive activation entropy ΔS^\ddagger of $19 \text{ JK}^{-1} \text{ mol}^{-1}$ suggests a more associative character of the transition state than in the reaction of cyanide with **1**. This behavior demonstrates that remote structural modifications of an anion receptor are not innocent but can be selectively used to alter the rate of binding.

CONCLUSIONS

We have synthesized three diastereomerically pure aquacyanocorrinoids and studied the substitution of cobalt-coordinated water with cyanide using stopped-flow measurements between 5 and 30 °C. The diastereomerically pure aquacyanocobinamides **1** and **2** exhibit second order rate constants of 23 and $72 \times 10^4 \text{ M}^{-1} \text{ s}^{-1}$ at 25 °C. Derivative **2** with a more shielded and deeper binding pocket reacts approximately 3 times faster. This behavior contradicts earlier studies suggesting indistinguishable rates for cyanide binding to diastereomeric aquacyanocorrinoids. The importance of the chemosensor's structure on the binding rate was also studied with corrin derivative **4** containing the same axial configuration at the metal center as **1** but distinct side chains at the periphery of the molecule. The presence of two methylester and one carboxylate functionalities instead of three acetamides lowers the rate by a factor of 3.5. Moreover, this structural change leads to a more associative character of the transition state as indicated by a less positive activation entropy.

In summary, these studies underscore that cyanide binding to metal complexes are affected by the configuration at the metal center as well as by the nature of remote side chains at the rim of the molecules. This behavior offers opportunities for tuning dynamic properties of chemosensors that are limited by slow anion binding dynamics in the future.

ASSOCIATED CONTENT

Supporting Information

NMR spectra, fitting KinTek Explorer, time-dependent absorption traces, along with a biexponential fit of these data (Figures S1–S4). This material is available free of charge via the Internet at <http://pubs.acs.org>.

AUTHOR INFORMATION

Corresponding Author

*E-mail: zelder@aci.uzh.ch. Website: www.felix-zelder.com.

Author Contributions

F.Z. planned experiments and wrote the manuscript. B.A. and C.C. conducted experiments, and B.A. performed the data analysis.

Notes

The authors declare no competing financial interest.

ACKNOWLEDGMENTS

The authors are grateful to the support by the Institute of Inorganic Chemistry of the University of Zurich and thank R. Alberto for helpful discussions. A generous gift of Vitamin B₁₂

from DSM Nutritional Products AG (Basel, Switzerland) is acknowledged.

REFERENCES

- (1) Martinez-Manez, R.; Sancenon, F. *Chem. Rev.* **2003**, *103*, 4419–4476.
- (2) Beer, P. D.; Gale, P. A. *Angew. Chem., Int. Ed.* **2001**, *40*, 486–516.
- (3) Santos-Figueroa, L. E.; Moragues, M. E.; Climent, E.; Agostini, A.; Martinez-Manez, R.; Sancenon, F. *Chem. Soc. Rev.* **2013**, *42*, 3489–3613.
- (4) Zelder, F. H.; Männel-Croise, C. *Chimia* **2009**, *63*, 58–62.
- (5) Xu, Z.; Chen, X.; Kim, H. N.; Yoon, J. *Chem. Soc. Rev.* **2010**, *39*, 127–137.
- (6) Gale, P. A.; Busschaert, N.; Haynes, C. J. E.; Karagiannidis, L. E.; Kirby, I. L. *Chem. Soc. Rev.* **2014**, *43*, 205–241.
- (7) Miyaji, H.; Sessler, J. L. *Angew. Chem., Int. Ed.* **2001**, *40*, 154–157.
- (8) Tomasulo, M.; Raymo, F. M. *Org. Lett.* **2005**, *7*, 4633–4636.
- (9) Gotor, R.; Costero, A. M.; Gil, S.; Parra, M.; Martinez-Manez, R.; Sancenon, F.; Gavina, P. *Chem. Commun.* **2013**, *49*, 5669–5671.
- (10) Hudnall, T. W.; Gabbai, F. P. *J. Am. Chem. Soc.* **2007**, *129*, 11978–11986.
- (11) Jose, D. A.; Elstner, M.; Schiller, A. *Chem.—Eur. J.* **2013**, *19*, 14451–14457.
- (12) Zelder, F. H. *Inorg. Chem.* **2008**, *47*, 1264–1266.
- (13) Panda, C.; Dhar, B. B.; Malvi, B.; Bhattacharjee, Y.; Gupta, S. S. *Chem. Commun.* **2013**, *49*, 2216–2218.
- (14) Ma, J. A.; Dasgupta, P. K. *Anal. Chim. Acta* **2010**, *673*, 117–125.
- (15) Divya, K. P.; Sreejith, S.; Balakrishna, B.; Jayamurthy, P.; Anees, P.; Ajayaghosh, A. *Chem. Commun.* **2010**, 6069–6071.
- (16) Männel-Croise, C.; Zelder, F. *Anal. Methods* **2012**, *4*, 2632–2634.
- (17) Männel-Croise, C.; Meister, C.; Zelder, F. *Inorg. Chem.* **2010**, *49*, 10220–10222.
- (18) Männel-Croise, C.; Probst, B.; Zelder, F. *Anal. Chem.* **2009**, *81*, 9493–9498.
- (19) Zhao, H.; Leamer, L. A.; Gabbai, F. P. *Dalton Trans.* **2013**, *42*, 8164–8178.
- (20) Lee, M. H.; Agou, T.; Kobayashi, J.; Kawashima, T.; Gabbai, F. P. *Chem. Commun.* **2007**, 1133–1135.
- (21) Kim, Y.; Gabbai, F. P. *J. Am. Chem. Soc.* **2009**, *131*, 3363–3369.
- (22) Männel-Croise, C.; Zelder, F. *Inorg. Chem.* **2009**, *48*, 1272–1274.
- (23) Zelder, F.; Alberto, R. In *The Porphyrin Handbook*; Kadish, K. M., Smith, K. M., Guillard, R., Eds.; Elsevier Science: San Diego, 2012; Vol. 25, pp 83–130.
- (24) Baldwin, D. A.; Betterton, E. A.; Pratt, J. M. S. *Afr. J. Chem.* **1982**, *35*, 173–175.
- (25) Chemaly, S. M.; Florczak, M.; Dirr, H.; Marques, H. M. *Inorg. Chem.* **2011**, *50*, 8719–8727.
- (26) Reenstra, W. W.; Jencks, W. P. *J. Am. Chem. Soc.* **1979**, *101*, 5780–5791.
- (27) Hamza, M. S. A.; Zou, X.; Banka, R.; Brown, K. L.; van Eldik, R. *Dalton Trans.* **2005**, 782–787.
- (28) Walker, D. T.; Dassanayake, R. S.; Garcia, K. A.; Mukherjee, R.; Brasch, N. E. *Eur. J. Inorg. Chem.* **2013**, 3049–3053.
- (29) Marques, H. M.; Bradley, J. C.; Brown, K. L.; Brooks, H. J. *Chem. Soc., Dalton Trans.* **1993**, 3475–3478.
- (30) Rakow, N. A.; Suslick, K. S. *Nature* **2000**, *406*, 710–713.
- (31) Chulvi, K.; Gavina, P.; Costero, A. M.; Gil, S.; Parra, M.; Gotor, R.; Royo, S.; Martinez-Manez, R.; Sancenon, F.; Vivancos, J.-L. *Chem. Commun.* **2012**, *48*, 10105–10107.
- (32) Männel-Croise, C.; Zelder, F. *ACS Appl. Mater. Interfaces* **2012**, *4*, 725–729.
- (33) Dale, T. J.; Rebek, J. *Angew. Chem., Int. Ed.* **2009**, *48*, 7850–7852.
- (34) Anzenbacher, P.; Liu, Y.; Palacios, M. A.; Minami, T.; Wang, Z.; Nishiyabu, R. *Chem.—Eur. J.* **2013**, *19*, 8497–8506.
- (35) Zhou, K.; Zelder, F. *Eur. J. Inorg. Chem.* **2011**, 53–57.
- (36) Zhou, K.; Zelder, F. *J. Porphyrins Phthalocyanines* **2011**, *15*, 555–559.
- (37) Pfammatter, M. J.; Darbre, T.; Keese, R. *Helv. Chim. Acta* **1998**, *81*, 1105–1116.
- (38) Zhou, K.; Zelder, F. *Eur. J. Inorg. Chem.* **2011**, 53–57.
- (39) *OriginPro*, 8.5.0 ed.; OriginLab Corporation: Northampton, MA, 2010.
- (40) *KinTek Explorer*, 4.0.2545 ed.; KinTek Corporation: Austin, TX, 2013.
- (41) Venkatesan, K.; Dale, D.; Hodgkin, D. C.; Nockolds, C. E.; Moore, F. H.; O'Connor, B. H. *Proc. R. Soc. London, Ser. A* **1971**, *323*, 455–487.
- (42) Kratky, C.; Farber, G.; Gruber, K.; Wilson, K.; Dauter, Z.; Nolting, H. F.; Konrat, R.; Kräutler, B. *J. Am. Chem. Soc.* **1995**, *117*, 4654–4670.